

A research on models of the photosynthetic light response curves on the example of evergreen types of plants

S. Korsakova¹, Yu. Plugatar¹, O. Ilnitsky¹ and M. Karpukhin²

¹FSBSI ‘The Labor Red Banner Order Nikita Botanical Gardens – National Scientific Center of Russian Academy of Sciences’ 298648, Russia, The Republic of Crimea, Yalta, urban vil. Nikita, Nikita Botanical Gardens

²Federal State Budget Educational Institution of Higher Education ‘Ural State Agrarian University’, 42, Karla Libknehta street, RU620075 Yekaterinburg, Sverdlovsk region, Russia

*Correspondence: Xoshyn@gmail.com

Abstract. The peculiarities of CO₂ exchange in the leaves of ornamental evergreen plant species that are common in the Southern coast of Crimea were studied: *Nerium oleander* L., *Laurus nobilis* L., *Aucuba japonica* Thunb., and *Melissa officinalis* L. The results of approximation of the most commonly used four models of P_N/I curves with the measured data were compared. The values of the parameters P_{gmax} , $\varphi_{(I_{comp})}$, R_D , I_{max} , which were calculated from the modified Michaelis-Menten model in comparison with the measured values were higher by 5–15%, and those that were calculated by the hyperbolic tangent model – lower by 3–13%. The use of a modified rectangular hyperbola model, which is capable of describing the photoinhibition by the nonrectangular hyperbola and the modified nonrectangular hyperbola model, showed a high degree of adequacy of the proposed models for describing the true dependence between the rate of photosynthesis and the light intensity for *Nerium oleander* L., *Laurus nobilis* L., *Aucuba japonica* Thunb. and *Melissa officinalis* L. Measurements of CO₂ exchange in leaves under similar environmental conditions showed significant differences in the parameters of the P_N/I curves: the light compensation point, the rate of photosynthesis and dark respiration, light saturation, and quantum yield. The highest values of photosynthesis efficiency were observed in *Nerium oleander*, the lowest values in *Aucuba japonica* – the light saturation was noted at a very low photosynthetically active radiation. The lower values of the light compensation point and the saturation constants in *Laurus nobilis* and *Aucuba japonica* indicate their effective use of the photosynthetically active radiation, which allows them to survive in conditions of durable shade.

Key words: evergreen species, CO₂ exchange, photosynthetic light response curves, fitting, nonlinear regression

INTRODUCTION

Many problems of plant physiology can be solved with proper completeness if quantitative methods are used in the studies (Drozdov et al., 2008). Studies in which we are using methods that do not violate the integrity of the plant have a particular relevance. One of such approaches is the construction of light dependences of CO₂ exchange, which

allows us to evaluate the efficiency of the use of light energy by the plant organism, incorporated in its genetic system, the mechanism of its utilization of light energy and the transformation of inorganic compounds of biogenic elements into organic substances (Zalensky, 1977; Zvalinsky, 2006). The analysis of the photosynthetic light-response curves (P_N/I curve) gives an important potential ecological and physiological characterization of this species, which allows us to compare different plant species growing in similar conditions of CO₂ exchange indicators; to receive important information about the adaptive mechanisms of the genotype, the plant diversity by competitiveness in such a narrow ecological niche, stress resistance and productivity (Kaibeyainen, 2009; Bolondinsky & Vilikainen, 2014). The use of methods of mathematical modeling contributes to the more detailed quantitative understanding of the mechanisms of plant functioning and their responses to external conditions (Thornley, 1982). Since there does not exist theoretically based solid model would be an ability to handle all experimental data of the real P_N/I curves,, currently, the number of models have been used to assess the relationship between the photosynthetic rate (P_N) and photosynthetically active radiation (PAR) are more than two dozen (Zvalinsky, 2006). Various experimental light curves are described by various functions: rectangular, nonrectangular hyperbola, Blackman's equation, exponential, hyperbolic tangent (Zvalinsky, 2006). All the curves have a similar shape, but they differ in the region of inflection and in achieving the maximum of photosynthesis. In the work of Lobo et al. (2013a), calculations of the statistical indices are presented and the method for selecting the approximating function of the P_N/I dependence by the method of least squares is shown (the error sum of squares, SSE) by means of add-in 'Solver' in 'Microsoft Excel 2010'.

The problems that a researcher encounters while quantitatively describing the real photosynthetic light curves, and the merits of the 'Statistica' system, which had analyzed the photosynthetic rate of light intensity in evergreen plant species growing in the Southern coast of the Crimea, are described in this paper.

The purpose of this work is to study the peculiarities of net CO₂ assimilation in leaves of ornamental evergreen plant species for the subsequent determination of their physiological differences in relation to the light factor. On the basis of experimental data, to examine the parameters of the photosynthetic light curve response models, to compare them with the measured data, determine the problems of each model using photosynthetic parameters calculated on the basis of the statistical function.

MATERIAL AND METHODS

Four evergreen plant species that are common in the landscaping of the Southern coast of the Crimea were used in the experiment: Oleander (*Nerium oleander* L.), Bay laurel (*Laurus nobilis* L.), Spotted laurel (*Aucuba japonica* Thunb.) and Lemon balm (*Melissa officinalis* L.).

Part of the experiments were carried out in a greenhouse of the Nikitsky Botanical Garden (NBG) under conditions of moderate shading (about 50–60% of total illumination), with the 4 year old seedlings, growing in 10-L vegetation vessels; another part of the experiments were in the field conditions with full sunlight, in the place of growth of the plants – in the upper park of the Arboretum Nikitsky Botanical Garden and the experimental area, located in the central branch of the NBG 'Lavrovoye'.

The maximal intensity of photosynthesis occurs in perennial evergreen plants after completion of leaf formation by its area and biomass (Tobias et al., 1995; Miyazawa & Terashima, 2001), so the intensity of carbon dioxide exchange of leaves was determined three times on well-developed intact leaves of the upper part of the plant shoot every 10–15 min using an automatic 4-channel open system for CO₂ exchange and leaf transpiration monitoring ‘Monitor photosynthesis RTM-48A’ (Bioinstruments S.R.L., Moldova) (Balaur et al., 2009). To measure the CO₂ exchange, a single-channel infrared gas analyzer (IRGA) with an open gas metering system by ‘PP Systems’ (USA) was used (Balaur et al., 2013). The CO₂ exchange is determined by decrement of CO₂ concentration at the outlet (C_{out}) of the leaf chamber, which is compared with the concentration of incoming ambient air (C_{in}). The CO₂ exchange rate (E) is calculated as follows: $E = k \times (C_{in} - C_{out}) \times F$, where F is air flow rate and k is a dimension factor, which depends on air temperature and pressure and is calculated automatically by the system. The standard air flow rate is 0.9 ± 0.1 liter per minute. The cycle starts from the pump switching on and leaf chamber connected to the analyzer channel. Within 1 min the channel of the leaf chamber is purging with ambient air; at the same time there is an automatic calibration for the gas analyzer, which lasts about 20 seconds. The reference concentration (C_{in}) is measured twice – at the end of this stage (C_{in1}) and after the closed chamber phase (C_{in2}). The arithmetic mean (C_{in}) of these two values is substituted in formula. In measurement cycle, the leaf is enclosed for 30 seconds only. An air pump provides an air stream from the circumference to the center of leaf chamber; then this air is fed through a connecting tube into the gas analyzer unit (Balaur et al., 2009). The leaf chamber was configured so that its elements did not obscure the leaf; the area of the window of the leaf chamber was 20 cm². The photosynthetically active radiation (PAR) and other environmental parameter, such as air temperature (in °C) and humidity (in %), were measured by the sensors of the RTH-48 Meteo module connected to the digital input of the RTM-48A system; leaf temperature (in °C) was measured with LT-1P leaf temperature sensor; soil moisture (in %) was measured with mineral soil sensor SMS-5M connected to the RTM-48A analog inputs. To obtain the P_N/I dependence, CO₂ exchange measurements were carried out in the PAR range from 0 to 2,000 μmol photons m⁻² s⁻¹, at the natural CO₂ concentration in the air of 0.04%. During experiments in the well-ventilated greenhouse the input gas for the CO₂ measurement was used the air of the greenhouse (at the CO₂ concentration in the air also of 0.04%).

Statistical processing of data was carried out in programs ‘Statistica 10’ (‘Statsoft Inc.’, USA) and ‘Microsoft Excel 2010’. All calculations were performed at a given significance level $P \leq 0.05$.

Experimental measurements in the field and in the greenhouse were carried out on sunny, mostly clear days in September 2015 and 2016. The investigated plants experienced neither a lack of soil moisture nor stress due to high temperature: the air temperature in the daytime varied within 26–31 °C, while that in the nighttime was within 19–24 °C, with the relative air humidity of 50–68% and soil moisture of 60–80% field capacity. The maximum measured value of PAR under treatment of full sunlight varied within 1,270–1,830 μmol photons m⁻² s⁻¹, under treatment moderate shading in greenhouse was within 470–630 μmol photons m⁻² s⁻¹.

Taking into account the frequency of application of the models (Jassby & Platt, 1976; Platt et al., 1977; Kaibeyainen, 2009; Dalke et al., 2013; Bolondinsky & Vilikainen, 2014), critical remarks, and the advantages of the proposed modern empirical

approaches and original projects (Thornley, 1982; Zvalinsky, 2006, Ye, 2007; Zvalinsky, 2008; Lobo et al., 2013b), in this study we compared the measured and the calculated photosynthetic parameters using four different well-described mathematical expressions of the P_N/I curve: the modified Michaelis-Menten model (Eq. 1) (Kaibeyainen, 2009), the hyperbolic tangent model (Eq. 2) (Jassby & Platt, 1976; Platt et al., 1977), the modified model of a rectangular hyper which can describe the photoinhibition by the nonrectangular hyperbola (Eq. 3) (Ye, 2007) and the modified model of the nonrectangular hyperbola (Eq. 4) (Zvalinsky, 2006, 2008).

$$P_N = \frac{IP_{gmax}}{I + I_{(50)}} - R_D, \quad (1)$$

$$P_N = P_{gmax} \tanh\left(\frac{\varphi_{(I_0)}I}{P_{gmax}}\right) - R_D, \quad (2)$$

$$P_N = \varphi_{(I_0-I_{comp})} \frac{1 - \beta I}{1 + \gamma I} (I - I_{comp}), \quad (3)$$

$$V = \frac{1 + [I]}{2\gamma_I} \left\{ 1 - \sqrt{1 - \frac{4\gamma_I[I]}{(1 + [I])^2}} \right\} \text{ where } V = P_N/P_{gmax} \text{ and } [I] = I/I_K \quad (4)$$

where P_{gmax} is the maximum of gross photosynthetic rate at the ‘optimal’ light intensity (below the level when the photoinhibition begins) (Zvalinsky, 2006), $\mu\text{mol CO}_2 \text{ m}^{-2} \text{ s}^{-1}$; P_N is the net photosynthetic rate, $\mu\text{mol CO}_2 \text{ m}^{-2} \text{ s}^{-1}$; R_D is the dark respiration rate, $\mu\text{mol CO}_2 \text{ m}^{-2} \text{ s}^{-1}$; I is the photosynthetically active radiation (PAR), $\mu\text{mol photons m}^{-2} \text{ s}^{-1}$; I_{comp} is the light compensation point (LCP) – the light intensity at which the total CO_2 exchange ($P_N/I_{(x,t)}$) equals zero, $\mu\text{mol photons m}^{-2} \text{ s}^{-1}$; $I_{(50)}$ is the point of light saturation for $P_N + R_D$, equal (50%) from P_{gmax} , $\mu\text{mol photons m}^{-2} \text{ s}^{-1}$; I_{sat} is the light saturation point, $\mu\text{mol photons m}^{-2} \text{ s}^{-1}$; I_k is the light constant, $\mu\text{mol photons m}^{-2} \text{ s}^{-1}$; $[I]$ is relative light intensity (dimensionless); $\varphi_{(I)}, \varphi_{(I_0)}, \varphi_{(I_{comp})}, \varphi_{(I_0-I_{comp})}$ are the quantum yield of photosynthesis (the tangent of the slope of the light curve, calculated as the derivative of P_N at point I) for different light intensities, for $I = 0$; $I = I_{comp}$; $I = I_0 - I_{comp}$, $\mu\text{mol CO}_2 \mu\text{mol photons}^{-1}$; β and γ are coefficients that are independent of irradiance (Ye, 2007), $\text{m}^2 \text{ s } \mu\text{mol photons}^{-1}$ and β is a correction factor for the decreasing trend of P_N when PAR exceed light saturation point due to photoinhibition and is similar to the convexity (Thornley, 1982), γ is a conversion factor for the initial slope of the P_N/I curve and the maximum photosynthetic rate; γ_I is the convexity factor (‘curvature’) of the non-rectangularity of the hyperbola, dimensionless.

Parameters P_{gmax} , R_D and I_{sat} for Eq. (3) were calculated from formulas (5–7) (Ye, 2007):

$$P_{gmax} = \varphi_{(I_0-I_{comp})} \frac{1 - \beta I_{sat}}{1 + \beta I_{sat}} (I_{sat} - I_{comp}) + R_D, \quad (5)$$

$$R_D = \varphi_{(I_0-I_{comp})} \cdot I_{comp}, \quad (6)$$

$$I_{sat} = \left(\sqrt{\frac{(\beta + \gamma)(1 + \gamma I_{comp})}{\beta}} - 1 \right) / \gamma. \quad (7)$$

The general forms of the P_N/I curve of Eqs (1)–(3) and calculation of the main photosynthetic characteristics ($\varphi_{(I)}$, I_{comp} , $I_{sat(n)}$) in ‘Excel’ (Eq. (5)–(15) developed by F.A. Lobo et al. (Lobo et al., 2013a, 2013b):

$$\varphi_{(I)} = \frac{I_{(50)} P_{gmax}}{(I + I_{(50)})^2}, \quad (8)$$

$$\varphi_{(I)} = \varphi_{(I_0)} \operatorname{sech}^2 \left(\frac{\varphi_{(I_0)} I}{P_{gmax}} \right) = \varphi_{(I_0)} \left[\frac{1}{\cosh^2 \left(\frac{\varphi_{(I_0)} I}{P_{gmax}} \right)} \right], \quad (9)$$

$$\varphi_{(I)} = \varphi_{(I_0 - I_{comp})} \frac{1 - \beta \gamma I^2 - 2\beta I + (\gamma + \beta) I_{comp}}{(1 + \gamma I)^2}, \quad (10)$$

$$I_{comp} = \frac{I_{(50)} R_D}{P_{gmax} - R_D}, \quad (11)$$

$$I_{comp} = \operatorname{arctanh} \left(\frac{R_D}{P_{gmax}} \right) \frac{P_{gmax}}{\varphi_{(I_0)}}, \quad (12)$$

$$I_{sat(n)} = \frac{I_{(50)} \left(R_D \frac{n}{100} - P_{gmax} \frac{n}{100} - R_D \right)}{P_{gmax} \left(\frac{n}{100} - 1 \right) + R_D \left(1 - \frac{n}{100} \right)}, \quad (13)$$

$$I_{sat(n)} = \operatorname{arctanh} \left[\frac{\frac{n}{100} (P_{gmax} - R_D) + R_D}{P_{gmax}} \right] \frac{P_{gmax}}{\varphi_{(I_0)}}, \quad (14)$$

$$I_{sat(n)} = \frac{AI_{comp} - B\gamma + C}{2A} - \frac{\sqrt{(B\gamma - AI_{comp} - C)^2 - 4A(CI_{comp} + B)}}{2A}, \quad (15)$$

$I_{sat(n)}$ in Eq. (13)–(15) is the light saturation point (LSP), determined at the photosynthesis rate $P_N + R_D$ equal (n%) from P_{Nmax} (Lobo et al., 2013a). To calculate any value of $I_{sat(n)}$, we can substitute the desired percentile value instead of (n) in the formula.

RESULTS AND DISCUSSION

Eq. (4) has three main parameters: the maximum rate of photosynthesis P_{gmax} , the light I_k constant and the non-rectitude parameter of the hyperbola γ_I (Zvalinsky, 2006, 2008). The parameter I_k (I -constant) is the main one for the light curve, the tangent of the slope angle $\varphi_{(I_0)}$ on its initial section is a dependent parameter. $I_k = P_{gmax} / \varphi_{(I_0)}$. $\varphi_{(I_0)} = a \times \varphi_{max}$ the a is the absorption, φ_{max} is the maximum quantum yield.

Theoretically, the maximum quantum yield is $0.1250 \mu\text{mol CO}_2 \mu\text{mol photons}^{-1}$, which means that 8 photons are required per one molecule of CO_2 fixed (Singsaas et al., 2001).

If we substitute V and $[I]$ with P_N/P_{gmax} and I/I_k , respectively, into Eq. (4), taking into account that $P_{gmax} = P_N + R_D$ (Ye, 2007), the photosynthetic rate will be equal to:

$$P_N = P_{gmax} \frac{I + I_k - \sqrt{(I + I_k)^2 - 4\gamma_I I I_k}}{2\gamma_I I_k} - R_D. \quad (16)$$

For any value of I in the set of the experimental data, an arbitrary quantum yield of photosynthesis φ_I is calculated as the derivative of the P_N/I curve in relation to I (Lobo et al., 2013a). The calculated derivative for the mathematical model (16) is presented in Eq. (17):

$$\varphi_{(I)} = \frac{P_{gmax}}{2\gamma_I I_k} \left(1 - \frac{I + I_k - 2\gamma_I I_k}{\sqrt{(I + I_k)^2 - 4\gamma_I I I_k}} \right). \quad (17)$$

When $I = 0$, Eq. (17) takes the next form:

$$\varphi_{(I_0)} = P_{gmax}/I_k. \quad (18)$$

Eq. (19) for calculation of the light compensation point I_{comp} from the model (16) was obtained after the transfer of the term I to the left side of the equation with the total CO_2 exchange equal to zero ($P_N = 0$):

$$I_{comp} = I_k R_D \frac{1 - \gamma_I \frac{R_D}{P_{gmax}}}{P_{gmax} - R_D}. \quad (19)$$

The general formula for calculating $I_{sat(n)}$ is obtained from the mathematical model (16), and is presented in Eq. (20):

$$I_{sat(n)} = \frac{I_k \left(\frac{n}{100} [R_D - R_{gmax}] - R_D \right) \left(1 - \gamma \left[\frac{\frac{n}{100} (P_{gmax} - R_D) + R_D}{P_{gmax}} \right] \right)}{\left(\frac{n}{100} - 1 \right) (P_{gmax} - R_D)}. \quad (20)$$

In addition to the main cardinal points of the light curve using the add-in ‘Solver’ in ‘Microsoft Excel 2010’, applying the Lobo approach (Lobo et al., 2013) for each model and species, we found the maximum light intensity I_{max} saturating P_N , as a point beyond which there is no significant increase in the rate of net photosynthesis. At this point, the maximum net photosynthetic rate saturated with light ($P_{N(I_{ma})}$) was calculated in the absence of photoinhibition. These variables are more realistic for representing the photosynthetic potential of plants, since their magnitude is always within the range of measurements (Lobo et al., 2013a). Taking into account the technical characteristics of the photosynthesis monitor RTM-48A (Balaur et al., 2009), the calculation of I_{max} was carried out if the maximum change in the measured values ΔP_N did not exceed $0.1 \mu\text{mol CO}_2 \text{ m}^{-2} \text{ s}^{-1}$ in the interval of light intensity increment $\Delta I = 50 \mu\text{mol photons m}^{-2} \text{ s}^{-1}$.

Module: Advanced Analysis / Nonlinear Estimation (Advanced Linear / Nonlinear Models) in the ‘Statistica’ system. Nonlinear estimation in the ‘Statistica’ system involves finding the best fit for the relationship between the values of the

dependent variable and the values of the set of one or more independent variables. Since the selection process is iterative, estimates of the primary parameters of the curve must be given. The initial estimates and ranges were based on our own experience with the study of species and the literature data. Only one initial guess of the free parameters was used. The maximum and minimum limits imposed for the parameters P_{gmax} , $\varphi_{(I_0)}$, R_D , LPC: the maximal rate of the net CO₂ uptake for C₃ species is up to 59 $\mu\text{mol CO}_2 \text{ m}^{-2} \text{ s}^{-1}$; the initial estimates of R_D obtained as approximately about 10% of P_{Nmax} , since both these estimates are interrelated (Lobo et al., 2013a); the maximum quantum yield is 0.1250 $\mu\text{mol CO}_2 \mu\text{mol photons}^{-1}$ (Singsaas et al., 2001); the LCP – from 2 to 150 $\mu\text{mol photons m}^{-2} \text{ s}^{-1}$ (Lobo et al., 2013a; Korsakova, et al., 2016); the range for the correction coefficients in Eq. (3) and the non-rectitude parameter of the hyperbola in Eq. (16) are from 0 to 1 ($0 < (\beta; \gamma; \gamma_1) < 1$) (Zvalinsky, 2006, 2008; Lobo et al., 2013a). The above indices help to choose the correct value for the parameters; however, the measured data are taken into account (Lobo et al., 2013a).

In order to determine the restrictions on the parameter change area, you should add to the loss function (in the ‘Loss function’ field) a penalty function equal to zero for the allowed values of the parameter and very large for invalid values. You can see an example below, which shows the input of a modified model of a rectangular hyperbola (Eq. (3) and the loss function including the imposition of a penalty if the parameter γ is less than or equal to zero:

The estimated function: $v2 = \varphi_{(I_0-I_{comp})} * ((1 - \beta * v1)/(1 + \gamma * v1)) * (v1 - I_{comp})$

The loss function: $L = (\text{OBS} - \text{PRED}) ** 2 + (\gamma \leq 0) * 100,000,000$

where $v1$ is the photosynthetically active radiation (I); $\mu\text{mol photons m}^{-2} \text{ s}^{-1}$; $v2$ is the net photosynthesis rate (P_N), $\mu\text{mol CO}_2 \text{ m}^{-2} \text{ s}^{-1}$.

In this paper to obtain the equations parameters, mathematical fitting of P_N/I curve models were performed with the Quasi-Newton method.

The user is given the complete control over all aspects of the evaluation procedure (initial values, step size, stopping criterion, etc.). The approximation of the model to the experimental dependence is considered to be best if the error sum of squares (SSE) of the desired analytic function from the experimental dependence is minimal. Even if the distribution of the dependent variable is not normal, the R^2 helps to evaluate how well the selected model is consistent with the original data (Stukach, 2011).

Comparison and experimental estimation of the model parameters. There is no single definitive universal mathematical model for application in all cases when describing real light curves; therefore, when carrying out specific studies, the best P_N/I curve from all existing ones will be the one that best corresponds to the initial data (Lobo et al., 2013a). Taking into account that the classical reaction of plant adaptation in response to changes in light conditions is characterized, as a rule, by changing the angle of inclination of the initial section of the light curve, the level of the light saturation plateau and the rate of the dark respiration, was carried out the comparative analysis of the consistency of approximating functions for P_N/I dependencies under different conditions of irradiance: under full sunlight and under moderate shading treatment (Fig. 1).

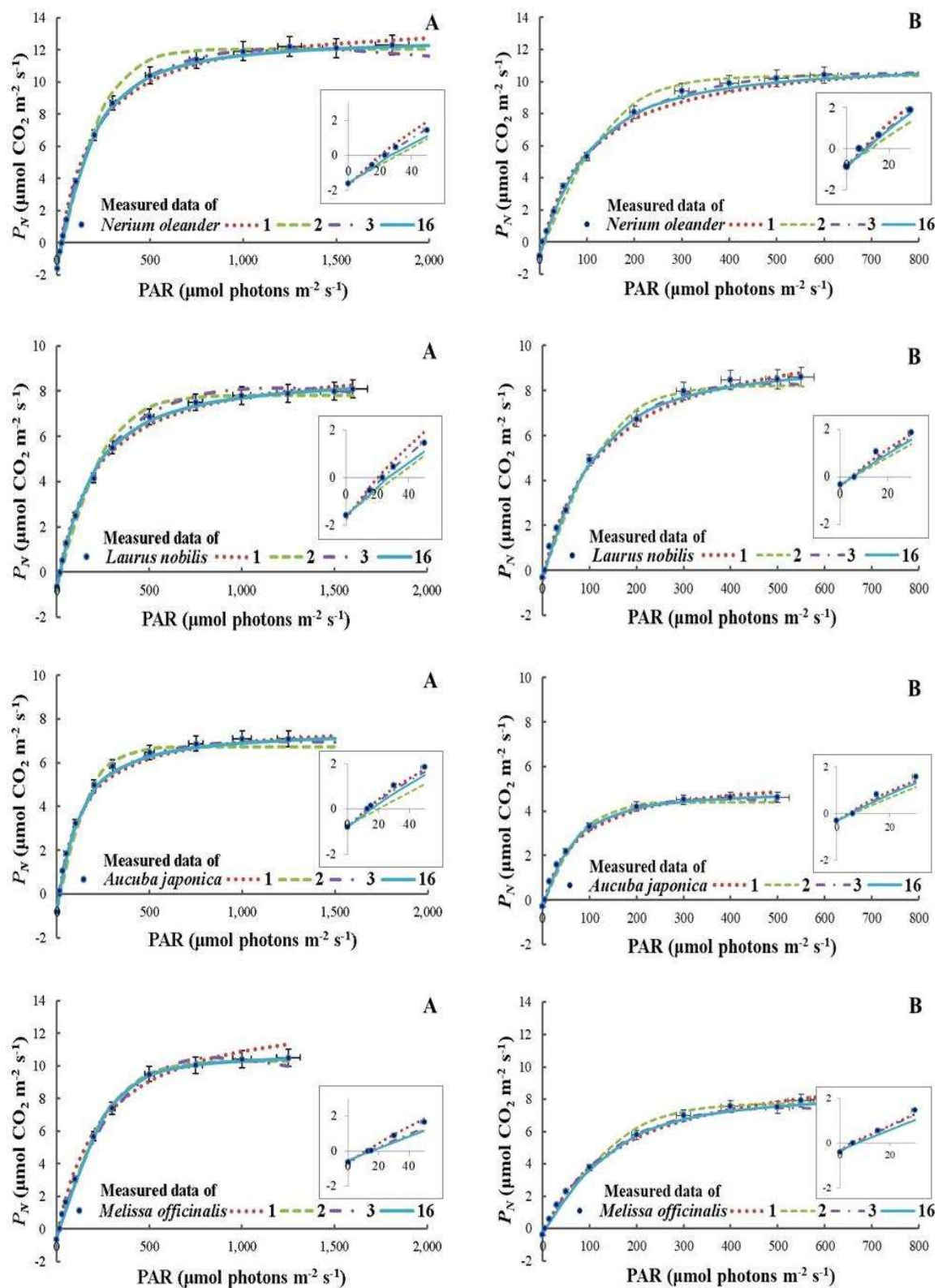


Figure 1. Fitting of the P_N/I curves using different mathematical models: A – full sunlight; B – moderate shading; 1, 2, 3, 16 – corresponding models of light response curves; P_N – net photosynthetic rate; PAR – photosynthetically active radiation.

Tables 1–4 show the average values and their standard deviations (\pm) of the experimental data, the parameters of the light curve models (Eqs (1), (2), (3) and (16), as well as the variables calculated from these models (Eqs (5)–(15), (17)–(20).

Statistical analysis showed that the P_N/I dependencies for *Nerium oleander*, *Laurus nobilis*, *Aucuba japonica* and *Melissa officinalis* are well described by the presented models (1), (2), (3) and (16) (Tables 1–4). The consistency of the calculated and measured data makes it possible to draw a conclusion about the adequacy of the studied models, which are in satisfactory coordination with each other. The check on the Student t-test of the regression coefficients showed that all the factors included in the model are significant at the 5% significance level. The parameters P_{gmax} , $\varphi_{(I_0-I_{comp})}$, R_D , I_{comp} , $I_{(50)}$ and I_K of the models of the light curves used in this study are highly significant ($p < 0.0001$). The significance level of the t-statistics of the correction coefficients γ and β (Eq. (3), as well as the ‘curvature’ γ_I index (Eq. (16) were predominantly within $p < 0.001$ – 0.05 , however, in about 40% of cases, the significance of the corrective coefficient of inhibition of photosynthetic reactions by light β (Eq. (3) were only at the 10–20% level (Korsakova et al., 2018). The resulting models of light curves of photosynthesis are characterized by a high degree of determination (the values of the determination coefficients were 94–99). In this study the mathematical model which fitted the best the measured data of P_N/I curve of *Nerium oleander* and *Laurus nobilis* was the modified rectangular hyperbola model (Eq. (3), Tables 1–2) because it had the lowest SSE. The best fitted for the measured data of P_N/I curve of *Aucuba japonica* and *Melissa officinalis* under full sunlight treatment was the modified rectangular hyperbola model (Eq. (3), Tables 3–4), under moderate shade treatment was the modified nonrectangular hyperbola model (Eq. (16), Tables 3–4). One of the reasons for the better coordination of these models with the experimental data are that equations (1) and (2) have constant values of internal convexity (‘curvature’), so they are not as universal as equations (3) and (16), with a variable parameter of the value of internal convexity (‘curvature’).

The parameter γ_I in Eq. (16) can take any value from 0 to 1 (Zvalinsky, 2006) so that it can be used to describe light curves of any curvature that have the same initial slope angle and maximum saturation level. At $\gamma_I = 0.0$, Eq. (16) becomes the equation of the rectangular hyperbola of Michaelis-Menten (Eq. (1)), and as the parameter increases to $\gamma_I \approx 0.999$ – the equation goes to the Blackman's broken line. The intermediate position is occupied by the function of the exponent ($\gamma_I \approx 0.8$) and the hyperbolic tangent ($\gamma_I \approx 0.95$) – Eq. (2) (Zvalinsky, 2006). The parameter γ_I has a clear biological meaning – the relative limitation of reactions beyond the limits of the substrate cycle. The high value of the parameter γ_I ($\gamma_I \approx 0.95$) means that the relative resistance of the substrate cycle (photochemical reactions of photosynthesis) is about 20 times lower (and the rate of these reactions is correspondingly 20 times higher) compared with the total resistance of reactions outside the substrate cycle (i.e. the dark reactions of photosynthesis and the ‘processing’ reactions) (Zvalinsky, 2008).

The modified Michaelis-Menten model (Eq. (1) with low internal convexity shows a relatively rapid decrease in the slope of the curve with increasing of I , which indicates a more gradual transition from light limitation to saturation, and leads to higher values of P_{gmax} and $\varphi_{(I)}$ in comparison with other models and initial data (Tables 1–4). The

models with low internal convexity have a very short quasilinear section and tend to give high values of $\varphi_{(I)}$ in the case when the initial data does show high convexity (Henley, 1993). The average value of the parameter P_{gmax} (Tables 1–4), found by Eq. (1), is the highest in comparison with other models, and by 7–10% higher than in accordance with Eq. (2).

One of the oldest and most used in the description of light dependencies is the parameter of saturating light intensity I_K (substrate light constant) which is equal to the value of light intensity at the intersection of the maximum photosynthetic rate and the line found by extrapolating the initial slope of the light curve. The parameter $I_K = P_{gmax}/\varphi_{(I_0)}$ was empirically introduced by J.F. Talling (Talling, 1957). The magnitude of the parameter I_K characterizes the light conditions, when photosynthesis is limited by the dark reactions under which the protective mechanisms begin to act, and can be used to evaluate the adaptive properties of the species (Gaevsky et al., 2012). The adaptation of the photophysical and photochemical stages to changes in the light regime determines the nature of the dark reactions of photosynthesis. A low I_K often indicates an ineffective use of the PAR, rather than an effective low utilization, and vice versa (Henley, 1993).

It should be noted that when using various functions in the description of light curves, the ratio between the value of the photosynthetic rate P_{gIk} at the point I_K and the maximum P_{gmax} will be different. When using an equation with a constant value of internal convexity ('curvature'), the ratio P_{gIk}/P_{gmax} (the mass fraction of light saturation of photosynthesis) is *const.* For example, when describing the P_N/I dependence by the Michaelis–Menten rectangular hyperbola function, the P_{gIk} rate will always reach 50% of the P_{gmax} ($P_{gIk}/P_{gmax} = 0.50$) at the I_K point, and if the hyperbolic tangent is $P_{gIk}/P_{gmax} = 0.76$ or 76% from P_{gmax} (see Tables 1–4). When using models with a variable parameter, the values of internal convexity ('curvature'), for example, in our studies this Eq. ((3) and (16), the ratio P_{gIk}/P_{gmax} is not constant, but can vary in the range from 0.50 to 1.00 (Tables 1–4).

In connection with the fact that a significant increase in photosynthesis is observed above I_K (Tables 1–4), quantitative equating I_K to light saturation is not justified. At the same time, this indicator actually approximately corresponds to light saturation, since it qualitatively determines the transition region from electron transfer control to carbon assimilation control (Henley, 1993).

In the proposed mathematical models, the main one is that P_{gmax} is the maximum specific rate of photosynthesis at the 'optimal' light intensity (below the level of irradiance when photoinhibition starts) (Zvalinsky, 2006). However, it should be taken into account that when describing the P_N/I dependence by the mathematical model of the hyperbola without taking into account the photoinhibition condition (Eqs (1) and (16), the P_{gmax} is the asymptote of the hyperbola as $I \rightarrow \infty$. In this case, the parameter P_{gmax} cannot be used as an independent variable to determine the maximum potential of photosynthetic species, since it does not exist in real life (Lobo et al., 2013a). In order to overcome the difficulty, a number of investigators suggested that the light saturation constant I_{sat} must be determined at a photosynthetic rate equal to 50% ($I_{sat(50)}$), 90% ($I_{sat(90)}$), 95% I_{sat} and 99% ($I_{sat(99)}$) from P_{gmax} or P_{Nm} (Kaibeyainen, 2009; Greer & Weedon, 2012; Lobo et al., 2013a). The maximum possible amount of the

photosynthetic active radiation reaching the Earth's surface is about 2,435 $\mu\text{mol photons m}^{-2} \text{ s}^{-1}$ (Jones et al., 2003) or slightly higher due to scattered radiation, which can increase this value. At higher altitudes, in connection with the tenuous air, higher values of the PAR can be observed. It is obvious that the values of I_{sat} above these maximum limits do not have a realistic eco-physiological meaning. From the statistical indices given in Tables 1–4, it can be seen that the values I_{sat} , obtained from equations (1) and (16) were higher than the maximum theoretically possible value that can reach Earth's surface or were out of the range employed to obtain the measurements.

Comparatively good comparability both with the results of measurements and with the results of calculations using the models (1), (2), (3) and (16), showed the maximum values of the parameter of saturating P_N at the light intensity of I_{max} – a point beyond which there is no significant changes in the net photosynthetic rate under the given conditions (Tables 1–4). A light-saturated rate of net photosynthesis ($P_{N(I_{max})}$) was found for this point. The results are consistent with the conclusion of F.A. Lobo (Lobo et al., 2013a) that I_{max} and $P_{N(I_{max})}$ more realistically represent the photosynthetic potential of a plant, their interpretation is immediate and obvious, since their values are always within the range of measurements.

The results of the studies given in Tables 1–4 show that the values of P_{gmax} , calculated using the modified Michaelis-Menten model (1), are on average 12–22% higher than using models (2), (3), and (16) and 15% higher than in the experimental data. Using the hyperbolic tangent model (model (2), this indicator, in comparison with other models, was on average 3–18% lower and 6% lower than the measured values.

The values of the visible quantum yield of photosynthesis $\varphi_{(I_{comp})}$ and dark respiration R_D , calculated from the model (1), compared to other models, were higher by an average of 18–60% and 5–15%, respectively, and calculated according to the model (2) – lower by 15–38% and 3–13%, respectively.

In comparison with the initial data, the average values of the parameters R_D and I_{max} , found from the function (1), exceeded the values measured in the experiments by 8% and 28%, respectively, and those calculated by the function (2), on the contrary, understated them by 65 and 19%, respectively. The position of the light compensation point I_{comp} on the light curve when using the model with low internal convexity (Michaelis-Menten model, Eq. (1), as a rule, was shifted to a lower irradiance field in comparison with the measured values by an average of 7%, and when using models with high internal convexity (hyperbolic tangent model, Eq. (2) – in the area of higher irradiance, on average by 20–30%. The difference between the values of this parameter, using Eq. (1) and Eq. (2), reached 30–40%.

One of the reasons for such discrepancies, both with the results of measurements and with the results of calculations for other models, is the variability of the real values of internal convexity ('curvature'), which is assumed constant in models (1) and (2).

Approximate values of the parameters P_{gmax} , $\varphi_{(I_{comp})}$, I_{comp} , R_D , I_{max} were obtained in the calculations using model equations (3) and (16). Their values on average did not differ by more than 5–13%. The average values of the photosynthetic indices, calculated using these model equations, in comparison with the values measured in the experiments, did not differ by more than 1–14% on average (Tables 1–4).

Table 1. Results fitted by four models P_N/I curve and measured data in *Nerium oleander* L. seedlings under different light conditions

Parameters	P_N/I models				Measured value
	(1)	(2)	(3)	(16)	
P_{gmax} ($\mu\text{mol CO}_2 \text{ m}^{-2} \text{ s}^{-1}$)	<u>15.6 ± 2.7</u> 12.8 ± 1.3	<u>13.6 ± 2.4</u> 11.1 ± 0.9	<u>14.1 ± 2.6</u> 11.5 ± 0.9	<u>14.4 ± 2.0</u> 12.2 ± 1.2	<u>14.7 ± 2.7</u> 12.3 ± 1.3
$\varphi_{(I_0)}$ ($\mu\text{mol CO}_2 \mu\text{mol photons}^{-1}$)	<u>0.10 ± 0.02</u> 0.13 ± 0.02	<u>0.05 ± 0.01</u> 0.07 ± 0.01	<u>0.08 ± 0.01</u> 0.11 ± 0.01	<u>0.06 ± 0.01</u> 0.10 ± 0.02	
$\varphi_{(I_{comp})}$ ($\mu\text{mol CO}_2 \mu\text{mol photons}^{-1}$)	<u>0.08 ± 0.02</u> 0.11 ± 0.03	<u>0.05 ± 0.01</u> 0.07 ± 0.01	<u>0.06 ± 0.01</u> 0.10 ± 0.02	<u>0.05 ± 0.01</u> 0.09 ± 0.02	
$\varphi_{(I_0-I_{comp})}$ ($\mu\text{mol CO}_2 \mu\text{mol photons}^{-1}$)			<u>0.07 ± 0.01</u> 0.10 ± 0.02		
R_D ($\mu\text{mol CO}_2 \text{ m}^{-2} \text{ s}^{-1}$)	<u>1.7 ± 0.2</u> 0.9 ± 0.3	<u>1.6 ± 0.2</u> 0.7 ± 0.3	<u>1.6 ± 0.1</u> 0.8 ± 0.3	<u>1.6 ± 0.1</u> 0.8 ± 0.3	<u>1.6 ± 0.1</u> 0.8 ± 0.2
I_{comp} ($\mu\text{mol photons m}^{-2} \text{ s}^{-1}$)	<u>20.3 ± 2.1</u> 7.9 ± 3.9	<u>31.2 ± 2.5</u> 11.6 ± 5.8	<u>23.6 ± 1.4</u> 8.6 ± 4.1	<u>26.5 ± 3.4</u> 9.6 ± 4.8	<u>23.3 ± 5.6</u> 5.8 ± 1.8
$I_{(50)}$ ($\mu\text{mol photons m}^{-2} \text{ s}^{-1}$)	<u>165 ± 7</u> 100 ± 6				
I_K ($\mu\text{mol photons m}^{-2} \text{ s}^{-1}$)	<u>165 ± 7</u> 100 ± 6	<u>269 ± 14</u> 164 ± 15	<u>163 ± 13</u> 101 ± 1	<u>253 ± 43</u> 128 ± 11	
I_{sat} ($\mu\text{mol photons m}^{-2} \text{ s}^{-1}$)			<u>1,387 ± 214</u> 918 ± 309		<u>880 ± 27</u> 440 ± 10
β ($\text{m}^2 \text{ s } \mu\text{mol photons}^{-1}$)			<u>0.0002 ± 0.0001</u> 0.0002 ± 0.0001		
γ ($\text{m}^2 \text{ s } \mu\text{mol photons}^{-1}$)			<u>0.004 ± 0.001</u> 0.007 ± 0.001		
γ_I				<u>0.71 ± 0.17</u> 0.55 ± 0.01	
P_{gIk} ($\mu\text{mol CO}_2 \text{ m}^{-2} \text{ s}^{-1}$)	<u>7.82 ± 1.33</u> 6.40 ± 0.66	<u>10.36 ± 1.85</u> 8.45 ± 0.66	<u>8.07 ± 1.75</u> 6.48 ± 0.69	<u>9.95 ± 2.69</u> 7.28 ± 0.65	
P_{gIk}/P_{gmax}	<u>0.50 ± 0.00</u> 0.50 ± 0.00	<u>0.76 ± 0.00</u> 0.76 ± 0.00	<u>0.57 ± 0.02</u> 0.56 ± 0.02	<u>0.68 ± 0.08</u> 0.60 ± 0.01	
I_{sat} ($\mu\text{mol photons m}^{-2} \text{ s}^{-1}$)	<u>2,815 ± 94</u> ¹ 1,773 ± 52	<u>509 ± 25</u> 306 ± 31	<u>782 ± 72</u> 488 ± 126	<u>1,600 ± 611</u> 1,249 ± 121	
I_{max} ($\mu\text{mol photons m}^{-2} \text{ s}^{-1}$)	<u>958 ± 34</u> 661 ± 87	<u>617 ± 15</u> 403 ± 1	<u>845 ± 21</u> 540 ± 24	<u>756 ± 59</u> 541 ± 84	
$P_{N(I_{max})}$ ($\mu\text{mol CO}_2 \text{ m}^{-2} \text{ s}^{-1}$)	<u>15.2 ± 2.8</u> 12.0 ± 1.1	<u>11.9 ± 2.4</u> 10.0 ± 1.4	<u>12.2 ± 2.8</u> 10.5 ± 1.2	<u>11.6 ± 2.3</u> 10.0 ± 1.6	<u>13.1 ± 2.6</u> 11.5 ± 1.5
SSE	<u>22.4 ± 26.4</u> 28.8 ± 10.4	<u>16.9 ± 16.9</u> 31.6 ± 9.2	<u>15.4 ± 17.8</u> 25.1 ± 7.6	<u>15.8 ± 18.3</u> 27.3 ± 9.8	

Designation: in the numerator – in the field under light treatments: full sunlight; in denominator – in greenhouse under light treatments: moderate shading; P_{gmax} – maximum gross photosynthetic rate; $\varphi_{(I_0)}, \varphi_{(I_{comp})}, \varphi_{(I_0-I_{comp})}$ – quantum yield of photosynthesis for different light intensities; R_D – dark respiration rate; I_{comp} – light compensation point; $I_{(50)}$ – point of light saturation for $P_N + R_D$, equal (50%) from P_{gmax} ; I_K – light constant; I_{sat} – light saturation point; β and γ – coefficients; γ_I – convexity factor, P_{gIk} – gross photosynthetic rate at the point I_K ; P_{gIk}/P_{gmax} – relative saturation of photosynthesis at the point I_K ; $I_{sat(9)}$ – light saturation point for photosynthetic rate of $P_N + R_D$, equals to 95% of P_{Nmax} ; I_{max} – light saturation point beyond which there is no significant increase in P_N ; $P_{N(I_{max})}$ – maximum net photosynthetic rate, calculated and measured at $I = I_{max}$; SSE – error sum of squares; 1 – $I_{sat(n)}$ estimates derived from Eqs. are higher than the maximum theoretical value that can reach Earth's surface; \pm – standard deviation.

Table 2. Results fitted by four models P_N/I curve and measured data in *Laurus nobilis* L. seedlings under different light conditions

Parameters	P_N/I models				Measured value
	(1)	(2)	(3)	(16)	
P_{gmax} ($\mu\text{mol CO}_2 \text{ m}^{-2} \text{ s}^{-1}$)	<u>10.1 ± 0.8</u> 11.2 ± 0.6	<u>8.5 ± 0.7</u> 8.5 ± 0.6	<u>8.7 ± 0.8</u> 8.7 ± 0.5	<u>9.6 ± 0.9</u> 9.8 ± 0.9	<u>9.2 ± 0.5</u> 9.3 ± 0.6
$\varphi_{(I_0)}$ ($\mu\text{mol CO}_2 \mu\text{mol photons}^{-1}$)	<u>0.05 ± 0.01</u> 0.09 ± 0.01	<u>0.03 ± 0.01</u> 0.06 ± 0.01	<u>0.04 ± 0.01</u> 0.08 ± 0.01	<u>0.04 ± 0.01</u> 0.07 ± 0.01	
$\varphi_{(I_{comp})}$ ($\mu\text{mol CO}_2 \mu\text{mol photons}^{-1}$)	<u>0.05 ± 0.01</u> 0.09 ± 0.01	<u>0.03 ± 0.01</u> 0.06 ± 0.01	<u>0.04 ± 0.01</u> 0.08 ± 0.01	<u>0.04 ± 0.01</u> 0.07 ± 0.01	
$\varphi_{(I_0-I_{comp})}$ ($\mu\text{mol CO}_2 \mu\text{mol photons}^{-1}$)			<u>0.04 ± 0.01</u> 0.08 ± 0.01		
R_D ($\mu\text{mol CO}_2 \text{ m}^{-2} \text{ s}^{-1}$)	<u>0.8 ± 0.4</u> 0.4 ± 0.1	<u>0.7 ± 0.3</u> 0.3 ± 0.1	<u>0.7 ± 0.3</u> 0.4 ± 0.1	<u>0.7 ± 0.4</u> 0.4 ± 0.1	<u>0.6 ± 0.2</u> 0.4 ± 0.1
I_{comp} ($\mu\text{mol photons m}^{-2} \text{ s}^{-1}$)	<u>16.5 ± 9.2</u> 4.6 ± 0.6	<u>25.1 ± 13.5</u> 5.5 ± 0.7	<u>19.0 ± 10.7</u> 4.9 ± 0.6	<u>19.5 ± 10.2</u> 5.2 ± 0.7	<u>16.3 ± 5.1</u> 5.9 ± 0.6
$I_{(50)}$ ($\mu\text{mol photons m}^{-2} \text{ s}^{-1}$)	<u>197 ± 29</u> 122 ± 13				
I_K ($\mu\text{mol photons m}^{-2} \text{ s}^{-1}$)	<u>197 ± 29</u> 122 ± 13	<u>295 ± 46</u> 150 ± 21	<u>201 ± 33</u> 111 ± 10	<u>234 ± 30</u> 140 ± 14	
I_{sat} ($\mu\text{mol photons m}^{-2} \text{ s}^{-1}$)			<u>1,190 ± 206</u> 493 ± 73		<u>737 ± 16</u> 343 ± 78
β ($\text{m}^2 \text{ s } \mu\text{mol photons}^{-1}$)			<u>0.0002 ±</u> <u>0.0001</u> 0.0005 ± 0.0001		
γ ($\text{m}^2 \text{ s } \mu\text{mol photons}^{-1}$)			<u>0.003 ± 0.001</u> 0.005 ± 0.001		
γ_I				<u>0.50 ± 0.10</u> 0.64 ± 0.09	
P_{gIk} ($\mu\text{mol CO}_2 \text{ m}^{-2} \text{ s}^{-1}$)	<u>5.06 ± 0.42</u> 5.62 ± 0.28	<u>6.48 ± 0.56</u> 6.51 ± 0.43	<u>5.10 ± 0.47</u> 5.35 ± 0.30	<u>5.62 ± 0.50</u> 6.17 ± 0.24	<u>5.06 ± 0.42</u> 5.62 ± 0.28
P_{gIk}/P_{gmax}	<u>0.50 ± 0.00</u> 0.50 ± 0.00	<u>0.76 ± 0.00</u> 0.76 ± 0.00	<u>0.59 ± 0.01</u> 0.61 ± 0.01	<u>0.59 ± 0.02</u> 0.63 ± 0.03	<u>0.50 ± 0.00</u> 0.50 ± 0.00
$I_{sat(9)}$ ($\mu\text{mol photons m}^{-2} \text{ s}^{-1}$)	<u>3,457 ± 406</u> ¹ 2,224 ± 240 ²	<u>554 ± 92</u> 278 ± 38	<u>719 ± 104</u> 319 ± 45	<u>2,466 ± 639</u> ¹ 1,105 ± 324	
I_{max} ($\mu\text{mol photons m}^{-2} \text{ s}^{-1}$)	<u>826 ± 85</u> 730 ± 51	<u>618 ± 82</u> 381 ± 43	<u>750 ± 95</u> 438 ± 54	<u>741 ± 90</u> 549 ± 87	
$P_{N(I_{max})}$ ($\mu\text{mol CO}_2 \text{ m}^{-2} \text{ s}^{-1}$)	<u>8.9 ± 1.0</u> 10.0 ± 0.4	<u>7.5 ± 0.4</u> 8.1 ± 0.6	<u>7.6 ± 0.4</u> 8.3 ± 0.6	<u>7.4 ± 0.4</u> 8.5 ± 0.7	<u>7.0 ± 0.4</u> 8.9 ± 0.4
SSE	<u>7.2 ± 2.5</u> 9.6 ± 1.1	<u>8.7 ± 3.3</u> 9.6 ± 0.6	<u>6.1 ± 2.1</u> 8.7 ± 0.9	<u>6.9 ± 2.4</u> 8.8 ± 0.8	

Designation: in the numerator – in the field under light treatments: full sunlight; in denominator – in greenhouse under light treatments: moderate shading; P_{gmax} – maximum gross photosynthetic rate; $\varphi_{(I_0)}$, $\varphi_{(I_{comp})}$, $\varphi_{(I_0-I_{comp})}$ – quantum yield of photosynthesis for different light intensities; R_D – dark respiration rate; I_{comp} – light compensation point; $I_{(50)}$ – point of light saturation for $P_N + R_D$, equal (50%) from P_{gma} ; I_K – light constant; I_{sat} – light saturation point; β and γ – coefficients; γ_I – convexity factor, P_{gIk} – gross photosynthetic rate at the point I_K ; P_{gIk}/P_{gmax} – relative saturation of photosynthesis at the point I_K ; $I_{sat(9)}$ – light saturation point for photosynthetic rate of $P_N + R_D$, equals to 95% of P_{Nmax} ; I_{max} – light saturation point beyond which there is no significant increase in P_N ; $P_{N(I_{max})}$ – maximum net photosynthetic rate, calculated and measured at $I = I_{max}$; SSE – error sum of squares; ¹ – $I_{sat(n)}$ estimates derived from Eqs. are higher than maximum theoretical value that can reach Earth's surface; ² – estimates of $I_{sat(n)}$ derived from Eqs. are out of range employed to obtain the measurements; \pm – standard deviation.

Table 3. Results fitted by four models P_N/I curve and measured data in *Aucuba japonica* Thunb. seedlings under different light conditions

Parameters	P_N/I models				Measured value
	(1)	(2)	(3)	(16)	
P_{gmax} ($\mu\text{mol CO}_2 \text{ m}^{-2} \text{ s}^{-1}$)	<u>8.7 ± 0.4</u> 5.9 ± 0.1	<u>7.5 ± 0.5</u> 4.7 ± 0.1	<u>7.8 ± 0.5</u> 4.9 ± 0.1	<u>8.3 ± 0.4</u> 5.3 ± 0.1	<u>8.2 ± 0.3</u> 6.3 ± 1.2
$\varphi_{(I_0)}$ ($\mu\text{mol CO}_2 \mu\text{mol photons}^{-1}$)	<u>0.07 ± 0.01</u> 0.09 ± 0.01	<u>0.04 ± 0.01</u> 0.05 ± 0.01	<u>0.07 ± 0.01</u> 0.07 ± 0.01	<u>0.06 ± 0.01</u> 0.06 ± 0.01	
$\varphi_{(I_{comp})}$ ($\mu\text{mol CO}_2 \mu\text{mol photons}^{-1}$)	<u>0.06 ± 0.01</u> 0.08 ± 0.01	<u>0.04 ± 0.01</u> 0.05 ± 0.01	<u>0.06 ± 0.01</u> 0.07 ± 0.01	<u>0.05 ± 0.01</u> 0.06 ± 0.01	
$\varphi_{(I_0-I_{comp})}$ ($\mu\text{mol CO}_2 \mu\text{mol photons}^{-1}$)			<u>0.06 ± 0.01</u> 0.07 ± 0.01		
R_D ($\mu\text{mol CO}_2 \text{ m}^{-2} \text{ s}^{-1}$)	<u>0.8 ± 0.1</u> 0.3 ± 0.1	<u>0.7 ± 0.1</u> 0.3 ± 0.1	<u>0.8 ± 0.1</u> 0.3 ± 0.1	<u>0.8 ± 0.1</u> 0.3 ± 0.1	<u>0.8 ± 0.1</u> 0.3 ± 0.1
I_{comp} ($\mu\text{mol photons m}^{-2} \text{ s}^{-1}$)	<u>12.1 ± 1.5</u> 4.3 ± 0.3	<u>19.6 ± 2.3</u> 6.0 ± 0.5	<u>13.3 ± 1.7</u> 4.8 ± 0.4	<u>15.1 ± 2.00</u> 5.2 ± 0.3	<u>12.6 ± 3.4</u> 6.0 ± 0.7
$I_{(50)}$ ($\mu\text{mol photons m}^{-2} \text{ s}^{-1}$)	<u>119 ± 4</u> 71 ± 5				
I_K ($\mu\text{mol photons m}^{-2} \text{ s}^{-1}$)	<u>119 ± 4</u> 71 ± 5	<u>199 ± 11</u> 95 ± 8	<u>119 ± 6</u> 67 ± 6	<u>152 ± 6</u> 83 ± 6	
I_{sat} ($\mu\text{mol photons m}^{-2} \text{ s}^{-1}$)			<u>$1,283 \pm 187$</u> 402 ± 47		<u>685 ± 93</u> 270 ± 20
β ($\text{m}^2 \text{ s } \mu\text{mol photons}^{-1}$)			<u>0.0001 ± 0.0001</u> 0.0005 ± 0.0001		
γ ($\text{m}^2 \text{ s } \mu\text{mol photons}^{-1}$)			<u>0.007 ± 0.001</u> 0.010 ± 0.002		
γ_1				<u>0.50 ± 0.03</u> 0.64 ± 0.07	
P_{gIk} ($\mu\text{mol CO}_2 \text{ m}^{-2} \text{ s}^{-1}$)	<u>4.34 ± 0.21</u> 2.97 ± 0.02	<u>5.69 ± 0.36</u> 3.58 ± 0.01	<u>4.28 ± 0.24</u> 2.87 ± 0.04	<u>4.87 ± 0.28</u> 3.32 ± 0.07	
P_{gIk}/P_{gmax}	<u>0.50 ± 0.00</u> 0.50 ± 0.00	<u>0.76 ± 0.00</u> 0.76 ± 0.00	<u>0.55 ± 0.01</u> 0.59 ± 0.02	<u>0.59 ± 0.01</u> 0.63 ± 0.02	
I_{sat} ($\mu\text{mol photons m}^{-2} \text{ s}^{-1}$)	<u>$2,065 \pm 98^2$</u> $1,266 \pm 99$	<u>375 ± 21</u> 177 ± 15	<u>643 ± 50</u> 240 ± 13	<u>$1,681 \pm 62$</u> 673 ± 154	
I_{max} ($\mu\text{mol photons m}^{-2} \text{ s}^{-1}$)	<u>624 ± 10</u> 413 ± 14	<u>453 ± 21</u> 244 ± 14	<u>600 ± 15</u> 312 ± 8	<u>572 ± 9</u> 323 ± 25	
$P_{N(I_{max})}$ ($\mu\text{mol CO}_2 \text{ m}^{-2} \text{ s}^{-1}$)	<u>8.1 ± 0.5</u> 5.4 ± 0.1	<u>6.6 ± 0.4</u> 4.3 ± 0.0	<u>6.6 ± 0.3</u> 4.5 ± 0.0	<u>6.4 ± 0.3</u> 4.5 ± 0.0	<u>6.5 ± 0.1</u> 5.6 ± 0.5
SSE	<u>8.5 ± 3.1</u> 8.4 ± 3.3	<u>10.5 ± 3.4</u> 8.4 ± 3.1	<u>8.1 ± 3.2</u> 7.8 ± 3.2	<u>8.2 ± 3.1</u> 7.76 ± 3.0	

Designation: in the numerator – in the field under light treatments: full sunlight; in denominator – in greenhouse under light treatments: moderate shading; P_{gmax} – maximum gross photosynthetic rate; $\varphi_{(I_0)}, \varphi_{(I_{comp})}, \varphi_{(I_0-I_{comp})}$ – quantum yield of photosynthesis for different light intensities; R_D – dark respiration rate; I_{comp} – light compensation point; $I_{(50)}$ – point of light saturation for $P_N + R_D$, equal (50%) from P_{gmax} ; I_K – light constant; I_{sat} – light saturation point; β and γ – coefficients; γ_1 – convexity factor, P_{gIk} – gross photosynthetic rate at the point I_K ; P_{gIk}/P_{gmax} – relative saturation of photosynthesis at the point I_K ; $I_{sat(9)}$ – light saturation point for photosynthetic rate of $P_N + R_D$, equals to 95% of P_{Nmax} ; I_{max} – light saturation point beyond which there is no significant increase in P_N ; $P_{N(I_{max})}$ – maximum net photosynthetic rate, calculated and measured at $I = I_{max}$; SSE – error sum of squares; ² – estimates of $I_{sat(n)}$ derived from Eqs. are out of range employed to obtain the measurements; \pm – standard deviation.

Table 4. Results fitted by four models P_N/I curve and measured data in *Melissa officinalis* L. seedlings under different light conditions

Parameters	P_N/I models				Measured value
	(1)	(2)	(3)	(16)	
P_{gmax} ($\mu\text{mol CO}_2 \text{ m}^{-2} \text{ s}^{-1}$)	<u>14.2 ± 0.3</u> 10.9 ± 1.4	<u>10.9 ± 0.5</u> 8.1 ± 0.7	<u>11.3 ± 0.6</u> 8.2 ± 0.6	<u>11.3 ± 0.2</u> 8.9 ± 0.6	<u>11.5 ± 0.2</u> 9.0 ± 0.8
$\varphi_{(I_0)}$ ($\mu\text{mol CO}_2 \mu\text{mol photons}^{-1}$)	<u>0.06 ± 0.01</u> 0.07 ± 0.01	<u>0.04 ± 0.01</u> 0.05 ± 0.01	<u>0.04 ± 0.01</u> 0.06 ± 0.01	<u>0.03 ± 0.01</u> 0.05 ± 0.01	
$\varphi_{(I_{comp})}$ ($\mu\text{mol CO}_2 \mu\text{mol photons}^{-1}$)	<u>0.06 ± 0.01</u> 0.06 ± 0.01	<u>0.04 ± 0.01</u> 0.05 ± 0.01	<u>0.04 ± 0.01</u> 0.06 ± 0.01	<u>0.03 ± 0.01</u> 0.05 ± 0.01	
$\varphi_{(I_0-I_{comp})}$ ($\mu\text{mol CO}_2 \mu\text{mol photons}^{-1}$)			<u>0.04 ± 0.01</u> 0.06 ± 0.01		
R_D ($\mu\text{mol CO}_2 \text{ m}^{-2} \text{ s}^{-1}$)	<u>0.7 ± 0.2</u> 0.4 ± 0.1	<u>0.5 ± 0.2</u> 0.3 ± 0.1	<u>0.6 ± 0.1</u> 0.4 ± 0.1	<u>0.5 ± 0.1</u> 0.3 ± 0.1	<u>0.6 ± 0.2</u> 0.4 ± 0.1
I_{comp} ($\mu\text{mol photons m}^{-2} \text{ s}^{-1}$)	<u>11.1 ± 2.0</u> 5.8 ± 0.9	<u>14.8 ± 3.7</u> 6.9 ± 1.6	<u>13.6 ± 3.5</u> 6.3 ± 1.3	<u>15.2 ± 4.4</u> 6.9 ± 1.7	<u>13.0 ± 3.3</u> 5.0 ± 1.0
$I_{(50)}$ ($\mu\text{mol photons m}^{-2} \text{ s}^{-1}$)	<u>231 ± 32</u> 163 ± 60				
I_K ($\mu\text{mol photons m}^{-2} \text{ s}^{-1}$)	<u>231 ± 32</u> 163 ± 60	<u>304 ± 12</u> 188 ± 50	<u>263 ± 22</u> 145 ± 48	<u>332 ± 16</u> 188 ± 66	
I_{sat} ($\mu\text{mol photons m}^{-2} \text{ s}^{-1}$)			<u>810 ± 13</u> 557 ± 64		<u>723 ± 18</u> 440 ± 53
β ($\text{m}^2 \text{ s } \mu\text{mol photons}^{-1}$)			<u>0.0004 ± 0.0001</u> 0.0005 ± 0.0001		
γ ($\text{m}^2 \text{ s } \mu\text{mol photons}^{-1}$)			<u>0.001 ± 0.001</u> 0.004 ± 0.002		
γ_1				<u>0.90 ± 0.04</u> 0.74 ± 0.12	
P_{gIk} ($\mu\text{mol CO}_2 \text{ m}^{-2} \text{ s}^{-1}$)	<u>7.10 ± 0.14</u> 5.46 ± 0.71	<u>8.26 ± 0.35</u> 6.15 ± 0.53	<u>7.49 ± 0.59</u> 5.19 ± 0.62	<u>8.70 ± 0.58</u> 6.07 ± 0.83	
P_{gIk}/P_{gmax}	<u>0.50 ± 0.00</u> 0.50 ± 0.00	<u>0.76 ± 0.00</u> 0.76 ± 0.00	<u>0.66 ± 0.01</u> 0.63 ± 0.04	<u>0.77 ± 0.04</u> 0.68 ± 0.07	
$I_{sat(95)}$ ($\mu\text{mol photons m}^{-2} \text{ s}^{-1}$)	<u>4,195±645¹</u> 2,990±1,116 ¹	<u>565±22</u> 347±93	<u>575±14</u> 370±47	<u>955±277</u> 940±210	
I_{max} ($\mu\text{mol photons m}^{-2} \text{ s}^{-1}$)	<u>1,072 ± 61</u> 799 ± 171	<u>670 ± 22</u> 440 ± 92	<u>725 ± 16</u> 484 ± 53	<u>680 ± 62</u> 530 ± 47	
$P_{N(I_{max})}$ ($\mu\text{mol CO}_2 \text{ m}^{-2} \text{ s}^{-1}$)	<u>12.4 ± 0.4</u> 9.5 ± 0.9	<u>10.1 ± 0.3</u> 7.6 ± 0.7	<u>10.7 ± 0.5</u> 7.8 ± 0.6	<u>10.0 ± 0.2</u> 7.8 ± 0.6	<u>10.8±0.3</u> 8.6±0.1
SSE	<u>39.5 ± 26.4</u> 19.4 ± 5.2	<u>34.9 ± 26.9</u> 19.0 ± 6.5	<u>34.4 ± 25.9</u> 17.9 ± 5.4	<u>35.1 ± 27.1</u> 17.8 ± 5.5	

Designation: in the numerator – in the field under light treatments: full sunlight; in denominator – in greenhouse under light treatments: moderate shading; P_{gmax} – maximum gross photosynthetic rate; $\varphi_{(I_0)}, \varphi_{(I_{comp})}, \varphi_{(I_0-I_{comp})}$ – quantum yield of photosynthesis for different light intensities; R_D – dark respiration rate; I_{comp} – light compensation point; $I_{(50)}$ – point of light saturation for $P_N + R_D$, equal (50%) from P_{gmax} ; I_K – light constant; I_{sat} – light saturation point; β and γ – coefficients; γ_1 – convexity factor, P_{gIk} – gross photosynthetic rate at the point I_K ; P_{gIk}/P_{gmax} – relative saturation of photosynthesis at the point I_K ; $I_{sat(95)}$ – light saturation point for photosynthetic rate of $P_N + R_D$, equals to 95% of P_{Nmax} ; I_{max} – light saturation point beyond which there is no significant increase in P_N ; $P_{N(I_{max})}$ – maximum net photosynthetic rate, calculated and measured at $I = I_{max}$; SSE – error sum of squares; ¹ – $I_{sat(n)}$ estimates derived from Eqs. are higher than the maximum theoretical value that can reach Earth's surface; ± – standard deviation.

The parameters of the P_N/I curve, obtained with the use of model Eqs (3) and (16) with a sufficient accuracy for practical purposes, correspond with each other and with direct measurements, and they can be used as a basis for calculating the dependence of photosynthetic rate on the light intensity for these species of evergreen plants. The proposed models have a high degree of adequacy to real P_N/I dependencies, however, it should be noticed that any model calculations grade a number of possible specific deviations, associated with the conditions of plant development or a sudden change in environmental conditions.

Fig. 2 shows the change in the quantum yield of photosynthesis of $\varphi_{(I)}$ in *Nerium oleander*, *Laurus nobilis*, *Aucuba japonica* and *Melissa officinalis*, depending on the photosynthetic photon flux density I under full sunlight (A) and moderate shading (B). $\varphi_{(I)}$ is calculated as a derivative of light curves models: model Eq. (1) – 1A, 1B; model Eq. (2) – 2A, 2B; the model Eq. (3) – 3A, 3B, and the model Eq. (16) – 16A, 16B. With increasing light intensity, the quantum yield decreased and reached zero at the point of light saturation. Comparison of the results of the calculations, presented in the Fig. 2, showed that at low intensities of I in the evaluated models, the values of $\varphi_{(I)}$ differ more than twofold (for example, 1AB and 2AB). Therefore, the search for the most accurate model becomes fundamentally important for the interpretation of all information. When evaluating the quantum yield, it should be taken into account that the values of $\varphi_{(I_0)}$ and $\varphi_{(I_0-I_{comp})}$, representing the ‘maximum quantum yield’, do not correspond to the original concept of this parameter, since photosynthesis is impossible in the dark. First of all, it is important to understand that $\varphi_{(I_0)}$ is the derivative of the model, when I equals zero. Secondly, nonlinear models do not have a ‘linear section’ in the literal sense of the word, so these sections can not be correctly inscribed in curvilinear dependencies, which in most cases are P_N/I dependencies. In this case, it is quite obvious that $\varphi_{(I_0)}$ is always the maximum value of the quantum yield, higher than any other point on the P_N/I curve. However, the $\varphi_{(I_0)}$ does not have a realistic value in terms of plant ecophysiology, since positive net assimilation in total darkness is impossible.

At the same time, the maximum visible quantum yield is the most accurate way to express the effectiveness of plant use of light in photosynthesis. It shows the amount of CO₂ bound during the photosynthesis process per one photon of light energy in the plant (Falkowski & Raven, 2007). The apparent quantum yield reflects the efficiency of the photosynthetic mechanism and affects the rate of photosynthesis, mainly at low and medium light intensities (Golovko, 1999). Since plant growth occurs most often under light that does not reach photosynthetic saturations, the magnitude of the apparent quantum yield can determine the rate of their primary production.

The magnitude of the visible quantum yield of photosynthesis is not constant, but varies depending on the conditions under which photosynthesis takes place. However, it is important to note that the relationship between the absorbed light and the O₂ release may differ from the ratio between the absorption of light and the absorption of CO₂. For ecophysiological purposes, it is preferable to use the term ‘apparent quantum yield’, since it does not use the light absorbed by the leaves, but the incident light, and no correction to eliminate the effect of photorespiration. (Singsaas et al., 2001). The maximum quantum yield appears to be better represented as the ratio of the net CO₂ evolution to the absorbed (or incident) light in the area of the P_N/I curve, where posi net

CO₂ assimilation begins (Ye, 2007). Depending on the emphasis, from the point of view of ecophysiological studies, it seems much more reasonable to use one theoretical maximum quantum yield ($\varphi_{(max)} = 0.125$) as a recommendation to determine how stress factors or specific conditions, affecting the plant, can affect the quantum yield or any other P_N/I parameter or calculated values (Golovko, 1999). This approach allows analyzing all points on the curve for ecophysiological purposes: if P_N is above the light compensation point, this means that there is net CO₂ absorption, the quantum yield values $\varphi_{(I)}$ can be analyzed not only when P_N depends on I , but also when P_N becomes increasingly independent of I . This possibility is very useful for assessing the differences in the efficiency of photosynthesis between sunny and shadow leaves, for which, not always, but often, there is no difference in $\varphi_{(I)}$ by the primary part of the P_N/I -curve. The slope of the linear portion of the light curve is primarily determined by the pigment content (Tarchevsky, 1977). In light species, the pigment content and the slope are usually at a less amount than in the shade-tolerant plants (Clayton, 1984).

Investigation of the parameters of light curves (Tables 1–4, Fig. 2) *Nerium oleander*, *Laurus nobilis*, *Aucuba japonica* and *Melissa officinalis* showed an increase in the efficiency of the use of light in moderate shade treatment, which indicates the adaptation of the photosynthetic mechanism to the growth conditions. Comparison of the dynamics of the quantum yield of photosynthesis in the irradiance range 0–100 $\mu\text{mol photons m}^{-2} \text{ s}^{-1}$, in Fig. 2, letters A and B, indicates an increase in the efficiency of using low light intensities by *Nerium oleander*, *Laurus nobilis*, *Aucuba japonica*, when there is deterioration of light conditions, which indicates a high degree of adaptation of the photosynthetic mechanism of these species to moderate shading. The absence of significant changes in the effectiveness of the CO₂ exchange of *Melissa officinalis* indicates that is sun plant with low-level activity of using low light intensities. With moderate shading, the intensity of respiration in the studied plant species decreased by 1.5–2.5 times on average, which can be regarded as a direct reaction to a decrease in the formation of assimilates due to the PAR decrease.

Analysis of photosynthesis light curve of *Nerium oleander*, *Laurus nobilis*, *Aucuba japonica* and *Melissa officinalis* showed that *Nerium oleander* possessed the photosynthetic apparatus characterized by a high rate of photochemical reactions (Table 1). The average value of the light compensation center *Nerium oleander* was in the range of 20–30 $\mu\text{mol photons m}^{-2} \text{ s}^{-1}$ under full sunlight; the light saturation was noted at PAR of 750–900 $\mu\text{mol photons m}^{-2} \text{ s}^{-1}$; the level of the dark respiration was at 1.6 $\mu\text{mol CO}_2 \text{ m}^{-2} \text{ s}^{-1}$, which indicates a light species. Shade-tolerant species generally have lower dark respiration rates and hence lower light compensation points (Loach, 1967), and lower light saturation points for photosynthesis than do shade-intolerant species (Pallardy, 2008). At the same time, the values of the angle of inclination of the initial section of the light curve and the parameter I_K indicate the ability of *Nerium oleander* to efficiently use light in photosynthesis in the low level of light intensities (160–250 $\mu\text{mol photons m}^{-2} \text{ s}^{-1}$ (Table 1).

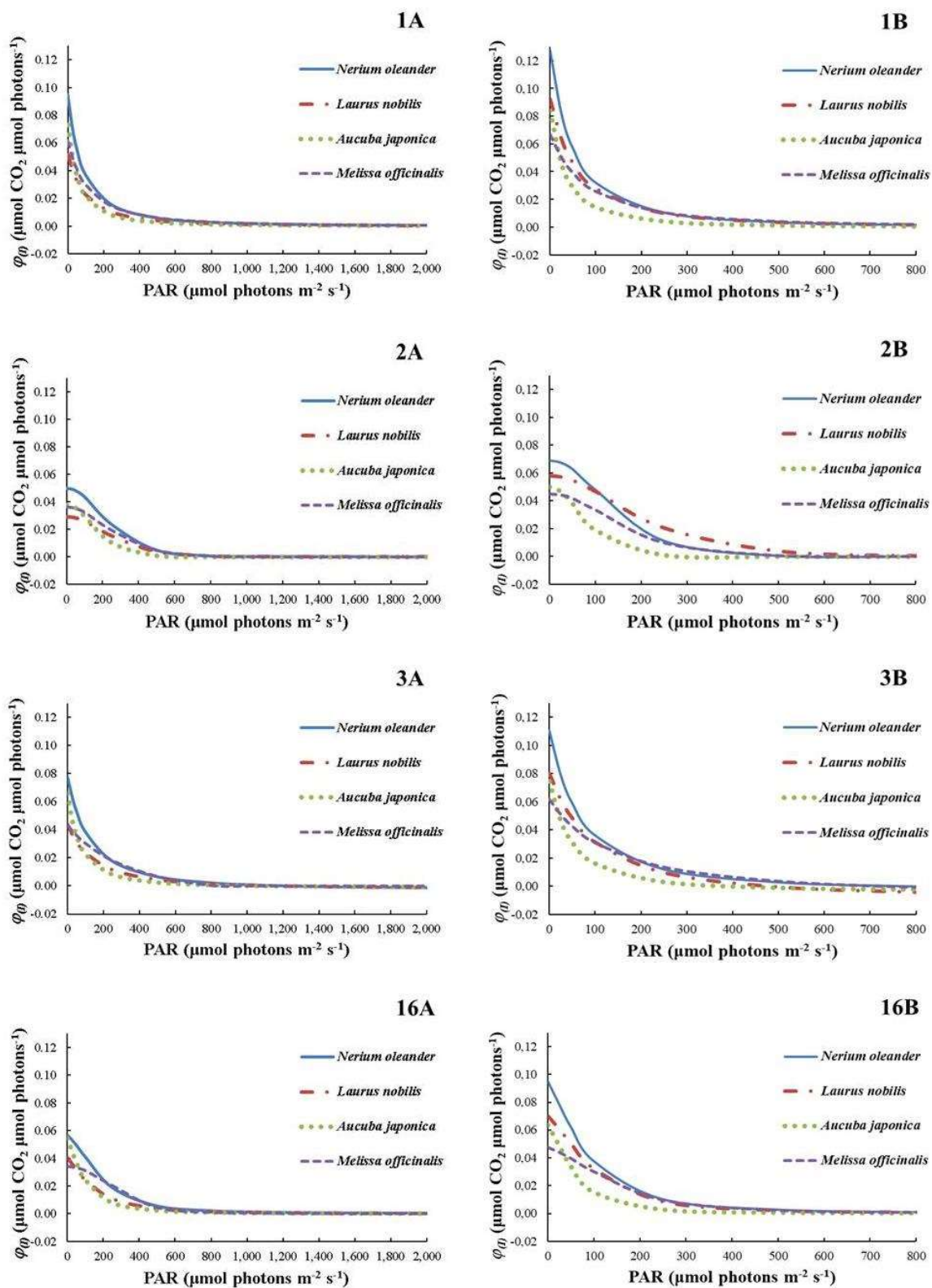


Figure 2. Dynamic curves of the quantum yield of photosynthesis) $A(\varphi_1)$ of *Nerium oleander*, *Laurus nobilis*, *Aucuba japonica* and *Melissa officinalis*: A – full sunlight; B – moderate shading; 1, 2, 3, 16 – derivatives of the corresponding models of light response curves; PAR – photosynthetically active radiation.

Moderate shading had a significant effect on the nature of the light curves of *Laurus nobilis*. With shading, the efficiency of the photosynthetic mechanism in the low values of PAR increased, which can be related to the formation of a more powerful pigment complex. The formation of the photosynthetic mechanism, adapted to shading, provided the ability of the leaves to maintain the rate of P_N not lower, but even higher than in plants under full sunlight (Table 2). Under conditions of moderate shading, the gross photosynthetic rate of leaves of P_{gIk} in the field of the light constant I_K was also higher than that of leaves under full sunlight. The intensity of the dark respiration decreased, which can be regarded as a direct reaction to a decrease in the formation of assimilates due to PAR reduction (Table 2). With moderate shading, the plants retained the intensity of growth of organic material due to an increase in the rate of photosynthesis. This was also facilitated by a slight decrease in the respiration rate of plants.

Based on the study of CO₂ exchange, it can be concluded that *Laurus nobilis* belongs to the group of light plants with well-marked signs of shadow tolerance. The presence of a flexible photosynthetic mechanism, the ability to function effectively in wide range of PAR, facilitate the adaptation of the species when growing on the Southern coast of the Crimea under conditions of intense insolation in open areas and under the canopy of plants of the first layer in conditions of predominance of diffuse radiation.

The most shade-tolerant of all the studied species was *Aucuba japonica*, which is characterized by the lowest activity of photosynthesis, a low rate of dark respiration, which most effectively uses low light intensities (Table 3, Fig. 2, A, B) both under full sunlight and under moderate shading. The light saturation of *Aucuba japonica*, in comparison with other species, occurred in weaker irradiance: under full sunlight treatment at 570–680 $\mu\text{mol photons m}^{-2} \text{ s}^{-1}$ PAR; under moderate shading conditions at 270–320 $\mu\text{mol photons m}^{-2} \text{ s}^{-1}$. The light constant I_K in this case decreased from 119–150 to 67–83 $\mu\text{mol photons m}^{-2} \text{ s}^{-1}$.

The light range that can provide the maximum of the photosynthetic intensity of *Melissa officinalis* is about 680–720 $\mu\text{mol photons m}^{-2} \text{ s}^{-1}$; the light constant I_K is at 260–330 $\mu\text{mol photons m}^{-2} \text{ s}^{-1}$; the slope of the initial segment of the light response curve is at 0.033–0.041 $\mu\text{mol CO}_2 \mu\text{mol photons}^{-1}$, which indicates its light species. Lower slope in the beginning it is a typical light response curve for a heliophytes plants (Blackman, 1905; Penning et al., 1989).

CONCLUSION

Under conditions of full sunlight and moderate shading significant differences in parameters P_{gmax} , $\varphi_{(I_{comp})}$, I_{comp} , R_D , I_{max} were found. The average values of the indices calculated from the four model equations differed from 2 to 60%, depending on the type of the parameter, and when compared with the measured data – from 1 to 30%. Values calculated by modified Michaelis-Menten model, overestimated the measured values of photosynthetic rates by 5–15%, and according by hyperbolic tangent model – understated the values by 3–13%. The highest level of consistency between the calculated and measured data for *Nerium oleander*, *Laurus nobilis*, *Aucuba japonica* and *Melissa officinalis* was observed using modified rectangular hyperbola model able to fit the photoinhibition stage by nonrectangular hyperbola and modified form of nonrectangular hyperbolic model.

The performed calculations allowed us to conclude that when using various functions to describe the photosynthetic response on the increase in the light flux even when using the same input values, the calculated characteristics for each individual function can differ significantly not only in absolute values, but also have opposite in signs in comparison with the experimental data, while maintaining a general tendency. Considering this fact in order to avoid distortion of the results of the parameters estimation when comparing plant species with relation to the light factor or when studying that relationship in the dynamics during the growing season, it is preferable to use one most suitable function for all investigation plant species.

These results of our studies are consistent with the findings of F.A. Lobo (Lobo et al., 2013a), where the variables I_{max} , $P_{N(I_{max})}$ and ϕ_1 better reflect the saturating light intensity, the maximum absorption rate of CO₂ at light saturation and the quantum yield of photosynthesis. They represent the photosynthetic potential of plants more realistically, because their values are always in the range of measurements.

Applying of methods, using the 'Statistica' system, can be an interesting alternative for users selecting the best light response curve of photosynthesis for the experimental data and its evaluation and interpretation of the results.

This new knowledge that we gained on physiological differences in relation to the light factor, provides valuable information on the adaptation of decorative plants that are have high potential for growing in the South coast of the Crimea, due to the light environment. This knowledge is important as potential ecological and physiological characteristic of these species when creating their ecological and physiological passports.

ACKNOWLEDGEMENTS. This study was supported by a research grant № 14-50-00079 of the Russian Science Foundation and founded by ST. 0829-2019-0021 of FSFIS 'NBG-NSC'.

REFERENCES

- Balaur, N.S., Vorontsov, V.A., Kleiman, E.I. & Ton, Yu.D. 2009. New technology for monitoring CO₂ exchange in plants. *Physiology of plants* **56**, 466–470 (in Russian).
- Balaur, N.S., Vorontsov, V.A. & Merenyuk, L.F. 2013. Features of photorespiration of photosynthetically active organs in C₃ plants. *Physiology of Plants* **60**(2), 174–183 (in Russian).
- Blackman, F.F. 1905. Optima and limiting factors. *Annals of Botany*. **9**, 281–295.
- Bolondinsky, V.K. & Vilikainen, L.M. 2014. Investigation of the light dependence of photosynthesis in the Karelian birch and silver birch under different conditions with different elements of mineral nutrition. *Proceedings of the Karelian Research Center of the Russian Academy of Sciences* **5**, 207–213 (in Russian).
- Clayton, R. 1984. *Photosynthesis. Physical Mechanisms and Chemical Models*. Mir, Moscow, 350 pp. (in Russian).
- Dalke, I.V., Butkin, A.V., Tabalenkova, G.N., Malyshev, R.V., Grigorai, E.E. & Golovko, T.K. 2013. Efficiency of the use of light energy in a greenhouse salad culture. *Izvestiya Timiriazevskaya Agricultural Academy* **5**, 60–68 (in Russian).

- Drozdov, S.N., Kholoptseva, E.S. & Popov, E.G. 2008. Nett photosynthesis of plants as an ecological indicator of biodiversity. In: *Fundamental and practical problems of botany in the early 21st century. Part 6: Ecological physiology and biochemistry of plants. Introduction of plants*. Karelian Research Center of the RAS, Petrozavodsk, pp. 47–49 (in Russian).
- Falkowski, P.G. & Raven, J.A. 2007. *Aquatic Photosynthesis*. Princeton University Press, Princeton, 488 pp.
- Gaevsky, N.A., Ivanova, E.A. & Dubrovskaya, M.A. 2012. Comparative evaluation of photosynthetic activity in a number of plants in Southern Siberia (Pearl Island, Republic of Khakassia). In: *Geoecological problems of steppe regions. The 6th Internacional Symposium*. IPK ‘Gazprompechat’ LLC ‘Orenburggazpromservis’, Orenburg, pp. 165–168 (in Russian).
- Golovko, T.K. 1999. *Respiration of plants (physiological aspects)*. Nauka, Leningrad, 204 pp. (in Russian).
- Greer, D.H. & Weedon, M.M. 2012. Modelling photosynthetic responses to temperature of grapevine (*Vitis vinifera* cv. Semillon) leaves on vines grown in a hot climate. *Plant, Cell and Environment*. **35**, 1050–1064.
- Henley, W.J. 1993. Measurement and interpretation of photosynthetic light-response curves in algae in the context of photoinhibition and diel changes. *J. Phycol.* **29**, 729–739.
- Jassby, A.D. & Platt, T. 1976. Mathematical formulation of the relationship between photosynthesis and light for phytoplankton. *Limnol. Oceanogr.* **21**, 540–547.
- Jones, H.B., Archer, N., Rotenberg, E. & Casa, R. 2003. Radiation measurement for plant ecophysiology. *J. Exp. Bot.* **54**, 879–889.
- Kaibeyainen, E.L. 2009. Parameters of the light response curve of photosynthesis in *Salix dasyclados* and their variation during vegetation. *Physiology of plants* **56**(4), 490–499 (in Russian).
- Korsakova, S.P., Ilnitsky, O.A. & Plugatar, Yu.V. 2016. Comparative evaluation of photosynthetic activity in some evergreen ornamental plants on the Southern coast of the Crimea. In: *Biotechnology as an Instrument for Plant Biodiversity Conservation (physiological, biochemical, embryological, genetic and legal aspects). The VII International Scientific and Practical Conference*. ARIAL, Simferopol, pp. 173.
- Korsakova, S.P., Ilnitsky, O.A. & Plugatar, Yu.V. 2018. Comparison of photosynthetic light-response curves models by the example of evergreen plant species. *Sc. in the south of Rus.* **14**(3), 88–100 (in Russian).
- Loach, K. 1967. Shade tolerance in tree seedlings. 1. Leaf photosynthesis and respiration in plants raised under artificial shade. *New Phytol.* **66**, 607–621.
- Lobo, F.A., Barros, M.P., Dalmagro, H.J., Dalmonin, Â.C., Pereira, W.E., Souza, É.C., Vourlitis, G.L. & Rodriguezortiz, C.E. 2013a. Fitting net photosynthetic light-response curves with Microsoft Excel – a critical look at the models. *Photosynthetica* **51**(3), 445–456.
- Lobo, F.A., Barros, M.P., Dalmagro, H.J., Dalmonin, Â.C., Pereira, W.E., Souza, É.C., Vourlitis, G.L. & Rodriguezortiz, C.E. 2013b. Erratum to: Fitting net photosynthetic light-response curves with Microsoft Excel – a critical look at the models. *Photosynthetica* **52**(3), 479–480.
- Miyazawa, S.-I. & Terashima, I. 2001. Slow Development of Leaf Photosynthesis in an Evergreen Broad-Leaved Tree, *Castanopsis sieboldii*: Relationships between Leaf Anatomical Characteristics and Photosynthetic Rate. *Plant Cell Environ.* **24**, 279–291.
- Pallardy, S. 2008. *Physiology of Woody Plants, 3rd ed.* Academic Press (Elsevier): Burlington, MA, USA, 453 pp.

- Platt, T., Denman, K.L. & Jassby, A.D. 1977. Modelling the productivity of phytoplankton. *The sea: ideas and observations of progress in the study of the seas*. N.Y.: John Wiley & Sons. **6**, 807–856.
- Penning de Vries, F.W.T., Jansen, D.M., Ten Berge, H.F.M. & Bakema, A. 1989. *Simulation of ecophysiological processes of growth in several annual crops*. Simulation Monographs, Pudoc, Wageningen, Netherlands, 271 pp.
- Singsaas, E.L., Ort, D.R. & DeLucia, E.H. 2001. Variation in Measured Values of Photosynthetic Quantum Yield in Ecophysiological Studies. *Oecologia* **128**, 15–23.
- Stukach, O.V. 2011. *The program complex 'Statistica' in solving problems of quality management: a textbook*. Publishing house of Tomsk Polytechnic University, Tomsk, 163 pp. (in Russian).
- Talling, J.F. 1957. Photosynthetic characteristics of some freshwater plankton diatoms in relation to underwater radiation. *New Phytol.* **56**, 29–50.
- Tarchevsky, I.A. 1977. *Fundamentals of photosynthesis*. Vysshaya shkola, Moscow, 254 pp. (in Russian).
- Thornley, J.H.M. 1982. *Mathematical models in plant physiology*. Naukova dumka, Kiev, 312 pp. (in Russian).
- Tobias, D.J., Ikemoto, A. & Nishimura, T. 1995. Leaf Senescence Patterns and Photosynthesis in Four Leaf Flushes of Two Deciduous Oak (*Quercus*) Species. *Photosynthetica* **31**, 231–239.
- Ye, Z.-P. 2007. A new model for relationship between irradiance and the rate of photosynthesis in *Oryza sativa*. *Photosynthetica* **45**(4), 637–640.
- Zalensky, O.V. 1977. *Ecological and physiological aspects of the study of photosynthesis. The 37th Timiryazev reading*. Nauka, Leningrad, 57 pp. (in Russian).
- Zvalinsky, V.I. 2006. Formation of primary production in the sea. *Izv. TINRO.* **147**, 277–304 (in Russian).
- Zvalinsky, V.I. 2008. Quantitative description of marine ecosystems. I. General approaches. *Izv. TINRO.* **152**, 132–153 (in Russian).